Polarized mitochondria as guardians of NK cell fitness

Laura Surace, Jean-Marc Doisne, Pedro Escoll, Solenne Marie, Valerie Dardalhon, Carys Croft, Anna Thaller, Davide Topazio, Angelo Sparaneo, Antonia Cama, et al.

HAL Id: pasteur-03162799

https://pasteur.hal.science/pasteur-03162799

Submitted on 8 Mar 2021

Polarized mitochondria as guardians of NK cell fitness

Laura Surace,[1,2] Jean-Marc Doisne,[1,2] Pedro Escoll,[3,4] Solenne Marie,[1,2] Valerie Dardalhon,[5] Carys Croft,[1,2,6] Anna Thaller,[1,2,6] Davide Topazio,[7] Angelo Sparaneo,[8] Antonia Cama,[9] Olimpia Musumeci,[10] Aurelio d'Ecclesia,[7] Carmen Buchrieser,[3,4] Naomi Taylor,[5] and James P. Di Santo[1,2]

[1]INSERM U1223, Paris, France; [2]Innate Immunity Unit and [3]Biology of Intracellular Bacteria Unit, Institut Pasteur, Paris, France; [4]UMR 3525, Centre National de la Recherche Scientifique (CNRS), Paris, France; [5]Institut de Génétique Moléculaire de Montpellier, University of Montpellier, CNRS, Montpellier, France; [6]BioSPC, Université de Paris, Paris, France; [7]Head and Neck Department, "Casa Sollievo della Sofferenza," Scientific Institute for Research and Health Care (IRCCS), San Giovanni Rotondo, Italy; [8]Laboratory of Oncology, "Casa Sollievo della Sofferenza," IRCCS, San Giovanni Rotondo, Italy; [9]Maxillofacial Surgery Unit, Department of Neuroscience, University Federico II, Naples, Italy; and [10]Unit of Neurology and Neuromuscular Disorders, Department of Clinical and Experimental Medicine, University of Messina, Messina, Italy

Key Points

- CD56^{Br} and CD56^{Dim} human NK cells have distinct bioenergetic requirements at steady state and upon activation.

- Mitochondrial dynamics and oxidative phosphorylation orchestrate NK cell function and fitness.

Distinct metabolic demands accompany lymphocyte differentiation into short-lived effector and long-lived memory cells. How bioenergetics processes are structured in innate natural killer (NK) cells remains unclear. We demonstrate that circulating human CD56^{Dim} (NKDim) cells have fused mitochondria and enhanced metabolism compared with CD56^{Br} (NKBr) cells. Upon activation, these 2 subsets showed a dichotomous response, with further mitochondrial potentiation in NKBr cells vs paradoxical mitochondrial fission and depolarization in NKDim cells. The latter effect impaired interferon-γ production, but rescue was possible by inhibiting mitochondrial fragmentation, implicating mitochondrial polarization as a central regulator of NK cell function. NKDim cells are heterogeneous, and mitochondrial polarization was associated with enhanced survival and function in mature NKDim cells, including memory-like *human cytomegalovirus*–dependent CD57$^+$NKG2C$^+$ subsets. In contrast, patients with genetic defects in mitochondrial fusion had a deficiency in adaptive NK cells, which had poor survival in culture. These results support mitochondrial polarization as a central regulator of mature NK cell fitness.

Introduction

Dynamic changes in energetic pathways govern lymphocyte maturation, activation, and long-term persistence. Naïve T cells reside in a resting basal metabolic state, where oxidative phosphorylation (OXPHOS) is sufficient to actively maintain the cells in quiescent state.[1] Proliferating T cells use glycolysis to keep up with ATP production and tricarboxylic acid cycle intermediates to favor the biosynthesis of materials that support division, differentiation, and cytokine production.[2,3] Long-lived memory cells increase fatty acid (FA) β-oxidation in a TRAF6-mediated prosurvival pathway.[1,4,5] Whereas changes in metabolic processes in T cells have been well studied, our knowledge of natural killer (NK) cell metabolism remains incomplete.

Human NK cells can be divided into 2 subpopulations based on differential expression of CD56 (NCAM) and CD16 (FcγRIIIA; low-affinity Fc receptor). In the blood of healthy donors (HDs), these subpopulations are identified as CD56^{Dim}CD16$^+$ NK (NKDim) cells, which are highly cytotoxic, and CD56^{Bright}CD16$^-$ NK (NKBr) cells, which are less cytotoxic but strong cytokine producers (interferon-γ [IFN-γ], tumor necrosis factor-α [TNF-α]).[6,7] NKBr and NKDim cells differentially express cytokine and homing receptors and show distinct tissue distributions.[6,8,9] Previous studies have begun to explore the metabolic requirements of resting and activated NK cells.[10-14] Peripheral blood NK cells increase

The full-text version of this article contains a supplement.

glycolysis and OXPHOS upon cytokine stimulation.[12] Specifically, upon interleukin-2 (IL-2)/12 stimulation, NKBr cells were reported to be metabolically more responsive compared with NKDim cells.[12] FA and glutamine pathways are upregulated in naïve NK cells[15]; however, excess of lipids blocks glycolysis, blunting NK cell antitumoral activity.[16] Overall, how environmental signals associated with NK cell survival and activation are integrated via reprogramming of intracellular energetic pathways remains unclear.

Mitochondria are highly dynamic organelles, shaped continuously by fusion and fission reactions.[17] Mitochondrial fusion, mediated by mitofusins and dynamin-like GTPase (OPA1), drives network formation, sustaining OXPHOS and cell survival,[18] whereas mitochondrial fragmentation is regulated by a cytosolic GTPase dynamin-related protein 1 and is associated with mitophagy.[19] Mitochondrial diseases (MDs) are rare inheritable disorders that include genetic mutations affecting mitochondrial structure, leading to impaired OXPHOS and decreased mitochondrial DNA integrity.[20,21] Although human adaptive NKG2C^{+} NK cells in *human cytomegalovirus (*HCMV)–exposed individuals have elevated mitochondrial OXPHOS,[10] it is not known whether altered mitochondrial dynamics impair NK cell differentiation. Here we analyzed how mitochondria regulate human NK cell homeostasis and function.

Materials and methods

Cell isolation from blood and tissue samples

Blood samples from HDs were obtained from the Establissement Francais du Sang (Paris, France). Tonsils were obtained from pediatric patients undergoing routine tonsillectomy ("Casa Sollievo della Sofferenza," Scientific Institute for Research and Health Care). Peripheral blood mononuclear cells (PBMCs) from MD patients were obtained from the Unit of Neurology and Neuromuscular Disorders at the University of Messina. Informed consent was obtained from all patients and included protocols approved by institutional review boards. Ficoll-Paque (GE Healthcare) was used for PBMC isolation, and cells were studied fresh (unless otherwise indicated). Tonsils were mechanically disrupted, and cells were frozen before use.

Cell culture

All in vitro culture experiments were performed in Yssel's medium.[22] Sorted cell were cultured in human IL-15 (50 ng/mL; Miltenyi), IL-12 (50 ng/mL; MBL), and IL-18 (50 ng/mL; R&D), provided in various combinations as indicated for 18 hours. To assess metabolic pathways, inhibitors were added during the 18 hours: 1 mM of [^{3}H] 2-deoxy-d-glucose (2-DG), 4 μM of bis-2-(5-phenylacetamido-1,3,4-thiadiazol-2-yl)ethyl sulfide (BPTES), 20 μM of etomoxir (ETO), 25 μM of mitochondrial division inhibitor 1 (Mdivi-1), 10 μM of rotenone (RO), 10 μM of antimycin A (AA), and 2 nM of oligomycin A (all from Sigma). For 12-day cultures, 5 μM of Mdivi-1 was used.

Flow cytometry and cell sorting

Cells were stained with surface antibodies and Flexible Viability Dye eFluor 506 (eBioscience) in phosphate-buffered saline/2% fetal calf serum for 30 minutes on ice. Surface glucose receptor 1 (GLUT-1) expression and glutamine receptor (ASCT2) expression were monitored as a function of binding to ligands as previously described.[23,24] For intracellular staining, cells were stimulated for 18 hours, and Golgi Plug/Golgi Stop (BD) were added for the last 3 hours. Cells were fixed/permeabilized using Cytofix/Cytoperm (BD) and then stained. Samples were acquired using the LSRFortessa (BD) and analyzed by FlowJ10 software (Tree Star). For cell sorting, PBMCs were lineage depleted using biotin-conjugated anti-CD3, anti-CD4, anti-CD19, anti-CD14, anti-CD123, and anti-CD235a (eBioscience) followed by antibiotin microbeads and AutoMACS separation (Miltenyi) according to the manufacturer's instructions. Cells were bulk sorted to a purity of ≥99% or single-cell index sorted (FACSAria II; BD) as previously reported.[22]

RNA isolation, library construction, sequencing, and analysis

A total of 10[3] NKDim (2 donors with 2 technical replicates) or NKBr cells (2 donors with no technical replicates) were sorted directly into 50 uL of lysis/binding buffer (Life Technologies). Messenger RNA was captured with 15 uL of Dynabeads oligo(dT) (Life Technologies) before washing and elution. Massively parallel single-cell RNA sequencing was performed as described.[22] Libraries were sequenced (Ilumina NextSeq) to an average depth of 5 million reads per library and aligned to the human reference genome (hg19). Reads were mapped using hisat (version 0.1.6); duplicate reads were filtered if they had identical unique molecular identifiers. Expression levels were calculated and normalized to the total number of reads using HOMER software (http://homer.salk.edu).

Cellular metabolism by seahorse extracellular flux analyzer

Oxygen consumption rates (OCRs) and extracellular acidification rates (ECARs) were measured for freshly sorted NK cells (200 000 cells) stimulated with IL-15 ± IL-12/18 (18 hours). XF media (containing 10 mM of glucose, 2 mM of L-glutamine, and 1 mM of sodium pyruvate) was used under basal conditions. Addition of 1 μM of oligomycin, 1.5 μM of carbonyl cyanide-4-(trifluoromethoxy)phenylhydrazone (FCCP), and 1 μM of RO + 1 μM of AA was performed using portal injection in an extracellular flux analyzer (Seahorse Bioscience).

Mitochondrial mass and membrane potential by fluorescence-activated cell sorting and confocal microscopy

Mitochondrial mass and membrane potential of freshly sorted or cytokine-activated NK cells were assessed by staining cells with 50 nM of MitoTracker Green FM (Thermo Fisher) and 25 nM of tetramethyl rhodamine methyl ester (TMRM; Sigma Aldrich), respectively, at 37°C for 30 minutes before surface staining. For confocal microscopy, nuclei of MitoTracker/TMRM-stained cells were counterstained with 300 ng/mL of Hoechst H33342 (Life Technologies). Cells were plated in 384-well plates (40 000 cells per well), and image acquisitions of multiple fields per well were performed on an automated confocal microscope (OPERA QEHS; Perkin Elmer) using 60× objectives, excitation lasers at 405, 488, and 561, and emission filters at 450, 540, and 600, respectively. Confocal images were transferred to the Columbus Image Data Storage and Analysis System (Perkin Elmer) for high-content analyses of mitochondrial morphology as previously reported,[25] and the standard deviation/mean approach was used for quantifying

mitochondrial membrane potential on confocal images using TMRM dye.[26]

Statistical analysis

Data are represented as medians unless specified. The sample size for each experiment and the replicate number of experiments are included in the figure legends as well as the specific test used for the analysis (Prism software).

Results

Monitoring metabolic profiles of NKDim and NKBr cells at steady state and after activation

To assess metabolic pathways that condition human NK cell responses, we compared characteristics of purified circulating NKBr (Lin⁻CD7⁺CD56^high CD16⁻CD127⁺) and NKDim cells (Lin⁻CD7⁺CD56^low CD16⁺CD127⁻; supplemental Figure 1A). Specifically, we compared freshly isolated NKBr and NKDim cells (steady state) with cells that underwent either IL-15 priming[27] or IL-12/IL-15/IL-18 activation[28-31] (Figure 1A).

Glucose and glutamine are key substrates of the mitochondrial bioenergetic pathways and have been reported to be essential nutrients for NK cell activation.[12,13,28] We therefore characterized GLUT-1 (*SLC2A1*) and ASCT2 (*SLC1A5*) expression in freshly sorted NKBr and NKDim cells. We found higher *SLC2A1* levels in NKDim cells, whereas *SLC1A5* expression was higher in NKBr cells (supplemental Figure 1B). These subset-specific differences were confirmed at the protein level, with a higher percentage of NKDim cells expressing GLUT-1 and NKBr cells expressing ASCT2 (Figure 1B; supplemental Figure 1C). IL-15–primed NKDim cells did not significantly upregulate either of these receptors, whereas the frequency of ASCT2⁺ NKBr cells increased after IL-15 exposure. NK cell activation (IL-12/18) enhanced the average expression levels of both receptors on both subsets. Although we did not detect any change in the already high percentage of ASCT2⁺ NKBr cells, we found increased frequencies of GLUT-1⁺ NKDim and NKBr cells as well as ASCT2⁺ NKDim cells after stimulation with IL-12 and IL-18 (Figure 1B).

We further studied nutrient receptors CD98 (a component of the L-amino acid transporter), CD71 (transferrin receptor), and CD36 (FA translocase). CD71 was expressed at higher levels in NKBr compared with NKDim cells at steady state; however, expression increased in response to cytokine stimulation for both subsets. CD98 and CD36 were upregulated in both subsets only upon activation (supplemental Figure 1C). Analysis of [³H]L-glutamine and 2-DG uptake showed increased uptake in both subsets upon priming and activation, with NKDim cells showing significantly greater glucose uptake than NKBr cells (supplemental Figure 1D). FAs are another important nutrient source that can fuel mitochondrial pathways. Because multiple FA transporters exist, we measured FA uptake using BODIPY-FLC16.[32] We found that upon activation, NKBr cells took up more long-chain FAs than NKDim cells (Figure 1C).

To clarify which of these various nutrients are required for NKBr and NKDim cells to exert their function, we studied the effects of inhibitors targeting glycolysis (2-DG), FA β-oxidation (ETO), and glutamine conversion into glutamate (BPTES). We found that IFN-γ and TNF-α were produced by NK cells only upon activation, and

NKBr cells produced higher levels of both cytokines compared with NKDim cells[15,27,29] (Figure 1D; supplemental Figure 1E). Treatment with 2-DG inhibited IFN-γ and TNF-α production by both NK cell subsets, consistent with a requirement for increased glucose uptake in this process. Although BPTES treatment did not alter the production of effector cytokines in either subset, both IFN-γ and TNF-α were significantly decreased in NKBr cells after treatment with ETO, suggesting that FA oxidation is important for NKBr cell activation and function (Figure 1D; supplemental Figure 1E). None of these inhibitors had an impact on NK cell viability (supplemental Figure 1F) or cytotoxic function (supplemental Figure 1G).

Distinct bioenergetics in NKBr and NKDim cells upon cytokine priming vs activation

We used the Seahorse bioanalyzer[33] to quantitate OCRs (indicator of OXPHOS) and ECARs (reflecting lactate production and glycolysis) in purified NK cell subsets. NKDim cells exhibited increased maximal ECARs after FCCP compared with NKBr cells (Figure 2A), indicating elevated maximal glycolysis capacity. NKDim cells also showed increased basal OCRs, higher maximal OCRs, and increased ATP-linked respiration when compared with NKBr cells (Figure 2B; supplemental Figure 2A), indicating that NKDim cells rely mainly on OXPHOS to produce ATP at steady state. SRC was higher in NKDim compared with NKBr cells (Figure 2C), consistent with latent mitochondrial capacity. RNA sequencing analysis confirmed that NKDim cells expressed higher levels of transcripts involved in OXPHOS compared with NKBr cells (Figure 2D; supplemental Figure 2B-D), providing a mechanistic explanation for the differential bioenergetics of these 2 NK cell subsets at baseline.
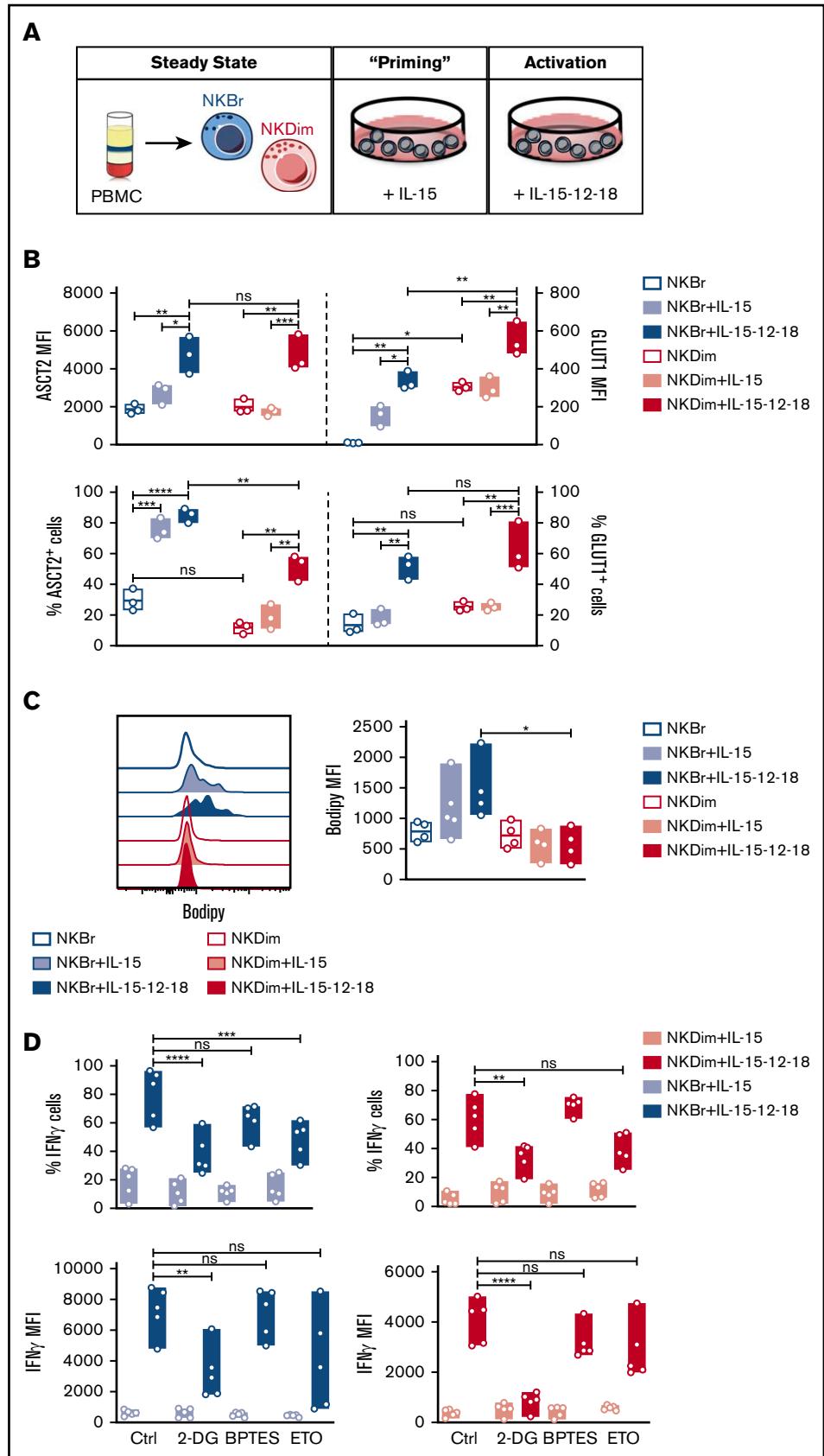
We next compared the impact of priming (IL-15) vs activation (IL-12/18) on the bioenergetics of these human NK cell subsets. NKDim cells maintained a high glycolytic rate after exposure to IL-15 (Figure 2E), whereas NKBr cells increased their aerobic capacity. After cytokine activation, both subsets showed higher maximal glycolysis (Figure 2E), consistent with the ability of these factors to promote NK cell proliferation and function. IL-15 induced a small increase in basal OCRs in NKDim cells, whereas maximal SRC remained stable (Figure 2F-G; supplemental Figure 2E), suggesting steady-state NKDim cells were already operating close to their bioenergetic limit. In contrast, IL-15–stimulated NKBr cells showed an increase in maximal OCRs and SCR, consistent with mitochondrial activation (Figure 2F-G). NKBr cells did not increase ATP-linked respiration, implying these cells might also rely on other pathways for ATP production (supplemental Figure 2E). In contrast, NK cell activation with IL-12/18 elicited a metabolic shift in NKDim cells, which showed decreased maximal OCRs, ATP-linked respiration, and SRC, whereas NKBr cells continued to have substantially large mitochondrial SRC (Figure 2F-G; supplemental Figure 2E). Cells with elevated SRC are more fit and have better survival capacity,[5,19,34] suggesting a fundamental difference in the bioenergetic stability of these 2 NK cell subsets after activation.

Distinct mitochondrial polarization patterns explain metabolic dichotomy in stimulated NKBr and NKDim cells

To explore the basis for the differences in metabolic profiles in cytokine-stimulated NKBr and NKDim cells, we further characterized mitochondrial mass and membrane polarization ($\Delta\psi_m$) using

Figure 1. Energetic substrate use in NKDim vs NKBr cells at steady state and upon activation. (A) In vitro model of NKBr and NKDim cell priming and activation. (B-D) Freshly fluorescence-activated cell-sorted NKDim and NKBr cells, IL-15 primed or activated with IL-15/12/18 (18 h) were monitored for cell-surface expression of the GLUT-1 and ASCT2 transporters and percentage of positive cells (B) (data from 3 independent experiments with 1 HD each) and FL-BODIPY-C16 uptake (C) (data from 3 independent experiments with 1 or 2 HDs each). (D) Expression of IFN-γ and percentage of IFN-γ–producing cells were monitored in NKBr and NKDim cells incubated with IL-15 or IL-15/12/18 for 18 hours in the presence of different inhibitors: 1 mM of 2-DG, 4 μM of BPTES, or 20 μM of ETO (data are mean ± standard error of the mean [SEM]; data summarized from 3 independent experiments with at least 2 HDs each). $P > .05$ was considered not significant (ns). $*P < .05$, $**P < .01$, $***P < .001$, $****P < .0001$ using 2-way analysis of variance with Tukey's correction. MFI, mean fluorescence intensity.
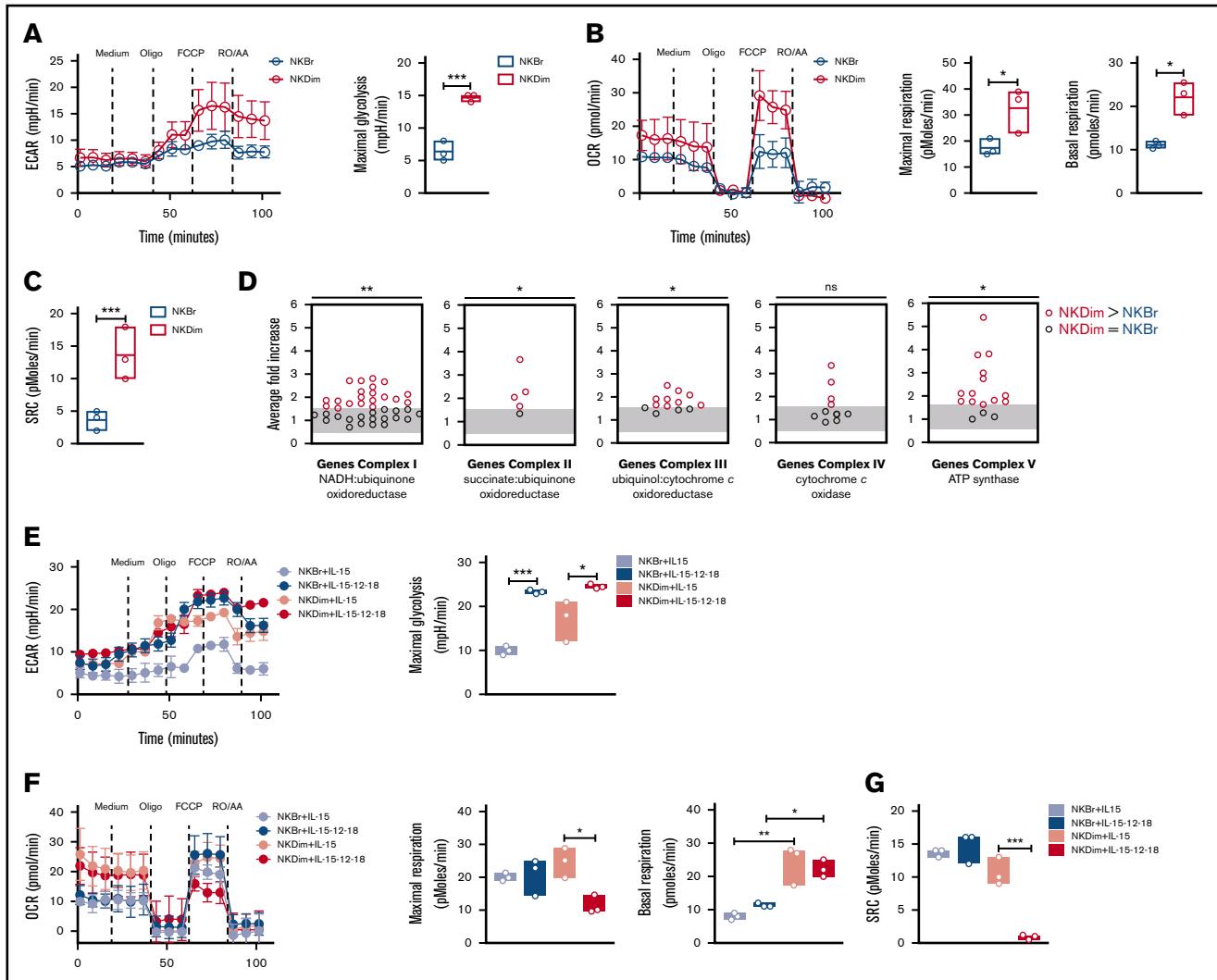
Figure 2. Steady-state CD56^Dim NK cells have latent mitochondrial activity and undergo a metabolic switch upon cytokine stimulation. (A-C) Metabolic function analyzed by extracellular flux analysis (EFA) in freshly fluorescence-activated cell-sorted (FACS) NKBr and NKDim cells. Cells were sequentially treated with glucose medium (medium), oligomycin A (Oligo), FCCP, and RO plus AA as indicated. (A) ECARs and maximal glycolysis (average values after glucose injection minus average basal ECAR values). (B) OCR plot. Calculation of the maximal respiration (average maximal OCR after FCCP) and basal respiration (average basal respiration after medium injection). (C) Mitochondrial spare respiratory capacity (SRC; average maximal OCR values after FCCP injection minus baseline OCR; data are representative of 3 independent experiments with 2 or 3 donors each). (D) Average fold increase comparing NKBr and NKDim cells is shown for all genes in OXPHOS complexes. Each dot represents the median relative expression level across donors. (E-G) EFA analysis in FACS NKBr and NKDim cells cultured for 18 hours in presence of IL-15 ± IL-12/18. Cells were sequentially treated as indicated above. ECAR and maximal glycolysis (E), OCR, maximal, and basal respiration (F), and SRC (G) (data are representative of 3 independent experiments; data are mean ± SEM). $P > .05$ was considered not significant (ns; or not indicated). *$P < .05$, **$P < .01$, ***$P < .001$ using 1-way analysis of variance with Tukey's correction.

MitoTracker Green FM and TMRM staining[19,25,35] (Figure 3; supplemental Figure 3A). We found that NKBr and NKDim cells had similar mitochondrial masses; however, NKDim cells showed higher TMRM levels and TMRM/MitoTracker ratios at steady state (Figure 3A-C). Single-cell and bulk gene expression analyses clearly demonstrated that TMRM^+ NKDim cells had an active OXPHOS and bioenergetic metabolism compared with TMRM^− cells (supplemental Figure 3B-D), suggesting NKBr cells exhibit a low energy state compared with NKDim cells.

Although mitochondrial mass did not change after IL-15 stimulation, both subsets showed an augmented $\Delta\psi_m$ (Figure 3A-C), consistent with the heightened levels of OXPHOS (Figure 2F). Because IL-15

primes NK cells in lymphoid tissues,[27] tissue-resident NK cells would be expected to have enhanced metabolic profiles compared with those in circulation. Tonsilar NK cells are largely enriched in NKBr cells[36] (supplemental Figure 3E-F) that have higher mitochondrial mass compared with both circulating subsets, with $\Delta\psi_m$ values similar to those of circulating NKDim cells at steady state (supplemental Figure 3G-H). These results suggest that tonsilar NK cells are metabolically primed.

IL-12 and IL-18 stimulation of blood NK cells did not affect mitochondrial mass (Figure 3A-C). Still, we detected a significant decrease in $\Delta\psi_m$ in NKDim cells but not in NKBr cells after activation (Figure 3A-C), in agreement with the Seahorse data
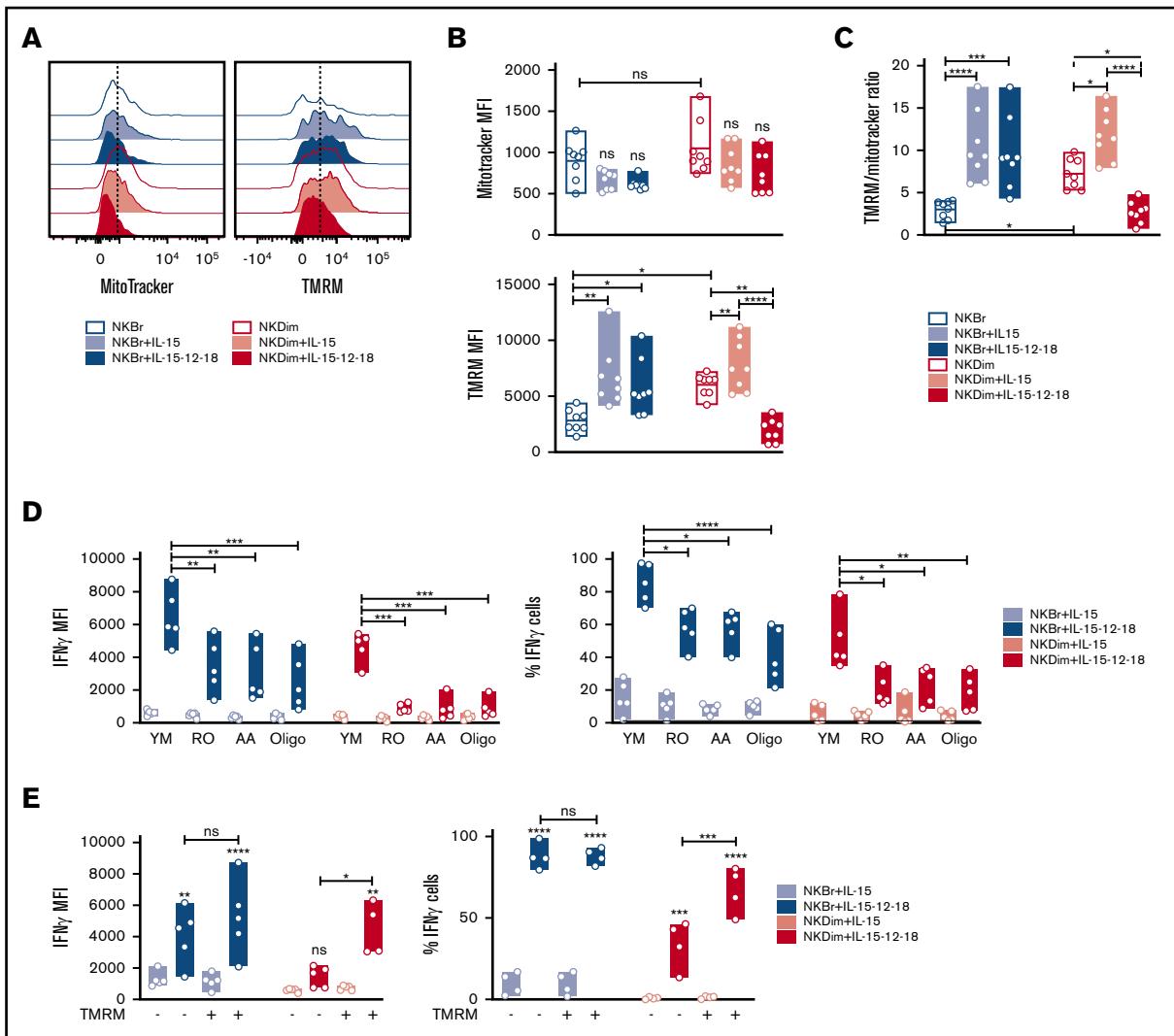
Figure 3. Mitochondrial membrane potential regulates cytokine production in cytokine-activated NK cells. (A-C) Mitochondrial mass was assessed by MitoTracker green and membrane potential ($\Delta\psi_m$) by TMRM incorporation in freshly sorted NKBr and NKDim cells (empty bars) and cultured for 18 hours in presence of IL-15 ± IL-12/18 (filled bars). (C) TMRM/Mitotracker ratio (data are mean ± SEM; data summarized from 4 independent experiments with 2 donors each). (D) Primed or activated NKBr and NKDim cells were cultured for 18 hours with the following inhibitors: 10 μM of RO, 10 μM of AA, and 2 nM of oligomycin A. Expression of IFN-γ and percentage of cells producing IFN-γ were monitored by fluorescence-activated cell sorting (FACS; data from 3 independent experiments with at least 2 donors each). (E) TMRM$^+$ and TMRM$^-$ NKBr and NKDim cells were sorted and cultured with IL-15 or IL-15/12/18 for 18 hours. Expression of IFN-γ and percentage of positive cells in the different conditions were measured by FACS (data from 4 HDs). $P > .05$ was considered not significant (ns). *$P < .05$, **$P < .01$, ***$P < .001$, ****$P < .0001$ using 1-way analysis of variance with Tukey's correction.

(Figure 2F-G). Addition of IL-12 or IL-18 alone to NK cells cultures did not affect mitochondria polarization, suggesting that a synergistic effect of the 2 cytokines is required to elicit the metabolic changes observed in NKDim cells (supplemental Figure 4A).

To assess the impact of OXPHOS on NK cells function, we used pharmacological inhibitors, including RO and AA, which inhibit complex I and complex III of the electron transport chain, respectively, and oligomycin A, which inhibits mitochondrial ATPase. At the concentrations used, these inhibitors showed no non-specific toxicity in culture (supplemental Figure 4B). We observed that RO, AA, and oligomycin A inhibited production of IFN-γ and TNF-α in NKBr cells (twofold) and to a larger extent in NKDim cells (eightfold; Figure 3D; supplemental Figure 4C). The same reduction was observed in the percentages of IFN-γ$^+$ and

TNF-α$^+$ NKDim and NKBr cells (Figures 3D and 4C), whereas no difference was reported in the cytotoxic markers tested in either subset (supplemental Figure 4D). Moreover, sorted and activated TMRM$^+$ NKDim cells showed increased IFN-γ production and percentage of IFN-γ$^+$ cells compared with TMRM$^-$ cells. No differences were observed comparing activated TMRM$^+$ and TMRM$^-$ NKBr cells (Figure 3E), demonstrating the importance of mitochondria polarization and OXPHOS in enhancing cytokine production, especially in NKDim cells.

Mitochondrial fragmentation and fusion govern NK cell function

Mitochondrial GTPases drive fission and fusion, which enhance glycolysis and OXPHOS, respectively.[17,25] We next characterized
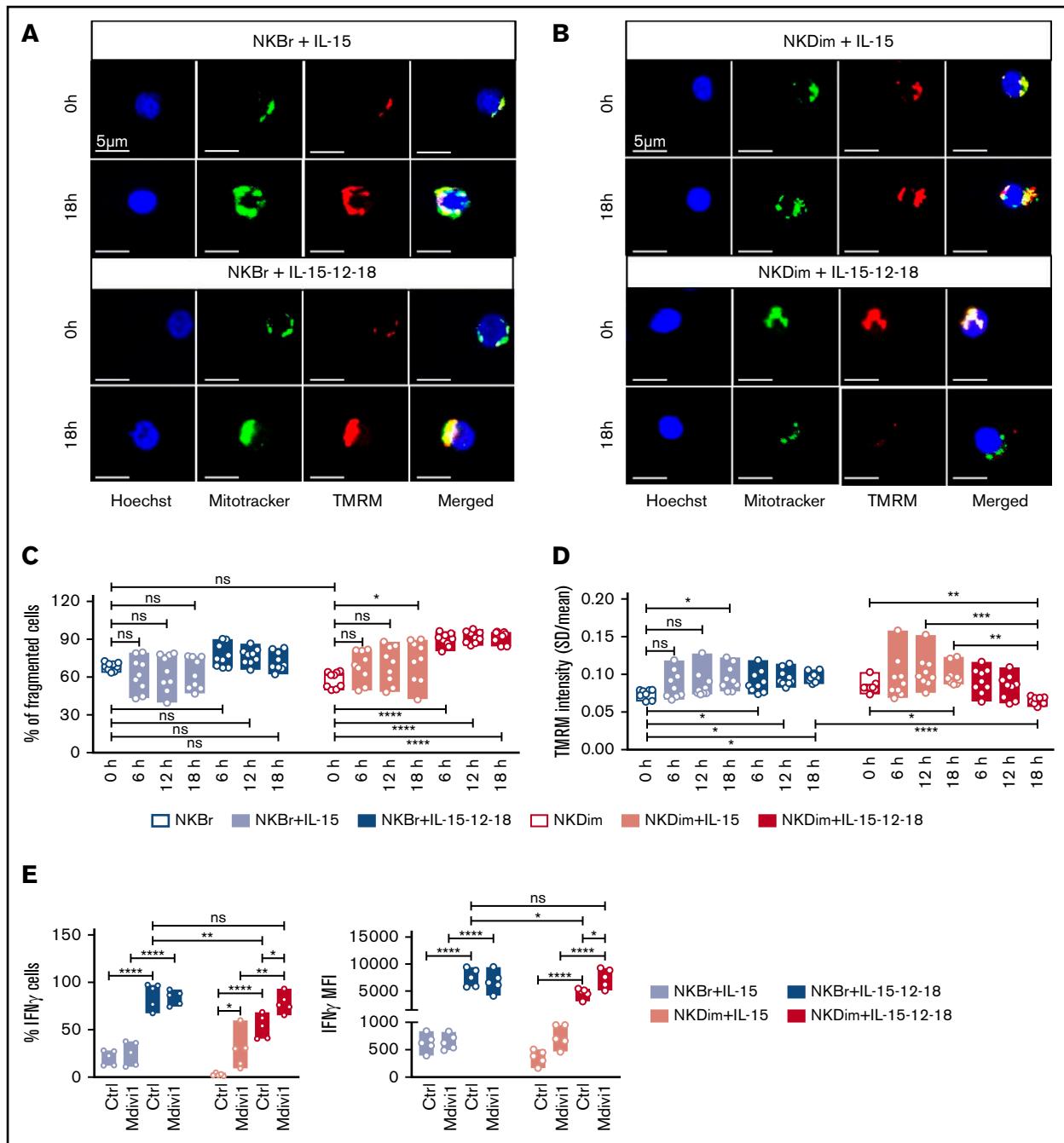
Figure 4. Divergent changes in mitochondrial morphology accompany activation of NKBr vs NKDim cells. (A-D) Freshly sorted NKDim and NKBr cells were stained with Mitotracker green and TMRM and imaged by confocal microscopy (0 hours). Cytokines were added to the medium as indicated in the figures, and images were taken every 6 hours. . (C-D) Mitochondrial fragmentation (C) and total TMRM intensity (D) at different time points for NKBr and NKDim cells. Circles are technical replicates from 3 HDs. (E) Primed or activated NKBr and NKDim cells were cultured for 18 hours ± Mdivi-1 (25 μM). Expression of IFN-γ was monitored by fluorescence-activated cell sorting; data from 3 independent experiments with at least 2 donors each). $P > .05$ was considered not significant (ns). *$P < .05$, **$P < .01$, ***$P < .001$, ****$P < .0001$ using 1-way analysis of variance with Tukey's correction.

mitochondrial morphology in freshly sorted, primed, and cytokine activated NKBr and NKDim cells by high-content confocal microscopy[25] (Figure 4A-D; supplemental Figure 5). We quantified TMRM-stained cells and confirmed previous reports[37] indicating TMRM intensity is higher in NK cells with nonfragmented mitochondria (supplemental Figure 5A).

We next analyzed changes in mitochondrial morphology in NKBr and NKDim cells upon cytokine stimulation (Figure 4A-D; supplemental Figure 5). NKDim and NKBr cells had comparable levels of mitochondrial fragmentation at steady state (Figure 4A-C), but after IL-15 priming, NKDim cells showed significantly more fragmented mitochondria, which was further accentuated after IL-12/18 exposure

(Figure 4B-C; supplemental Figure 5B). In contrast, NKBr cells did not show any significant changes in mitochondrial fragmentation after cytokine priming or activation (Figure 4A,C; supplemental Figure 5C). Thus, the mitochondrial response in NKBr and NKDim cells during priming and activation was dichotomous: NKDim cells increased mitochondrial polarity upon IL-15 priming but fragmented their mitochondria after activation, whereas NKBr cells maintained fused and polarized mitochondria after priming and activation (Figure 4A-D; supplemental Figure 5B-C).

We next examined the effect of Mdivi-1, a selective inhibitor of mitochondrial fragmentation, on NK cell function. Mdivi-1 increased mitochondria polarization in NK cells (supplemental Figure 6A) and had no apparent nonspecific toxicity (supplemental Figure 6B). Mdivi-1 significantly increased IFN-γ and TNF-α production by IL-15–primed NKDim cells and IL-12 + IL-18–activated NKDim but not NKBr cells (Figure 4E; supplemental Figure 6C), consistent with the previously observed dichotomous response. Mdivi-1 had no effect on cytotoxicity-related parameters in either subset (supplemental Figure 6D). These results show that mitochondrial dynamics differ in NKBr and NKDim cells and that mitochondrial fusion promotes OXPHOS and cytokine production by NKDim cells.

Mitochondrial polarization is associated with cellular fitness and effector function in NKDim cells

The dichotomous mitochondrial response to IL-12/18 stimulation observed in NKDim cells suggests that the effector capacity of these cells may be short lived. Nevertheless, a subset of long-lived memory NK cells has been described after exposure to HCMV[38-40] and other chronic infections.[41] Multiple studies, along with our data, have shown that mitochondrial fusion and OXPHOS improve overall cellular fitness and function.[5,19,34]

Interestingly, frequencies of TMRM^{+} NK cells in the blood of healthy individuals were highly variable and largely confined to the NKDim compartment (Figure 5A). Within NKDim cells, TMRM expression was enriched in more mature CD57^{+} cells[8] and also significantly increased within the NKG2C^{+}NKG2A^{-} subset (Figure 5B-C; supplemental Figure 7A-B) that is expanded in HCMV^{+} individuals.[38-40] When comparing HCMV^{-} and HCMV^{+} individuals, we found that TMRM expression was highly upregulated in CD57^{+}NKG2C^{+}NKG2A^{-} NK cells as previously reported[10] (Figure 5B-C; supplemental Figure 7A-B). Still, we found elevated mitochondrial $\Delta\psi_m$ within CD57^{+}NKG2C^{-}NKG2A^{-} but not CD57^{+}NKG2C^{-}NKG2A^{+} NKDim cells (supplemental Figure 7A-B), suggesting that mitochondrial polarization and OXPHOS are not unique features of the NKG2C^{+} subset but may rather mark fully matured NK cells.

To determine whether the mitochondrial polarization associated with HCMV exposure imprints survival and functional advantages on NKDim cells, we isolated total NKDim cells from HCMV[+] and HCMV[-] donors and stimulated them under priming or activation conditions. We observed that HCMV^{-} NKDim cells proliferated extensively upon stimulation with activating cytokines before abruptly dying at ~day 6 (Figure 5D). In contrast, HCMV^{+} NKDim cells showed slower expansion, but cells persisted until the experimental end point (Figure 5D), consistent with the presence of fused mitochondria. To improve cellular fitness in HCMV^{-} NKDim cells, we added Mdivi-1 to the cultures and observed improved expansion levels, although still reduced compared with stimulated

HCMV^{+} NKDim cells (Figure 5D), suggesting Mdivi-1 could partially rescue mitochondrial fragmentation in cytokine-stimulated HCMV^{-} NKDim cells, thereby blocking cell death.

As expected, CD57^{+}NKG2C^{+}NKG2A^{-} cells were highly enriched in stimulated HCMV^{+} NKDim cultures (Figure 5E); however, NKG2C^{+} cells accounted for only 50% of total cells, indicating that other subsets (not expressing NKG2C) can expand upon long-term stimulation. Moreover, expanded HCMV^{-} NKDim cells treated with Mdiv-1 remained NKG2C^{-} (Figure 5E), demonstrating that Mdivi-1–induced survival did not convert CD57^{+}NKG2C^{-}NKG2A^{-} NKDim to NKG2C^{+} NKDim cells. An analysis of the function showed that surviving NKDim cells at day 12 could produce high levels of IFN-γ irrespective of HCMV status (Figure 5F). These results indicate that Mdivi-1 can partially restore not only survival but also function of HCMV^{-} NKDim cells (Figure 5F). CD107a and cytotoxic markers were at comparable levels in HCMV[-] and HCMV^{+} NKDim cells (Figure 5G; supplemental Figure 7C).

NK cells from OPA1-deficient patients have less polarized mitochondria, reduced cellular fitness, and impaired memory-like NK cell homeostasis

We studied MD patients with an OPA1 missense mutation (A495V) to better understand the role of mitochondrial fusion in NK cell homeostasis. Compared with HDs, MD patients had similar percentages of NKBr but lower frequencies of NKDim cells (Figure 6A). Concerning the percentages of TMRM^{+} cells, we did not find any effect on NKBr cells, whereas TMRM^{+} NKDim cells were reduced in MD patients compared with HDs (Figure 6B). As expected, MD patients showed lower overall levels of TMRM uptake; however, NKDim homeostasis seemed more strongly dependent on OPA1 function.

We further analyzed the phenotype of NKDim cells in MD patients. In this cohort, all patients were HCMV^{+} by serological analysis; we therefore compared them with HCMV^{+} and HCMV^{-} HDs. As expected,[42] the percentages of CD57^{+} NKDim cells were higher in HCMV^{+} donors and similar between MD patients and HDs (Figure 6C). However, MD patients had lower percentages of CD16^{+} cells and striking deficiency in CD57^{+}NKG2C^{+}NKG2A^{-} compared with HCMV^{+} HDs (Figure 6C). This result suggests that maintenance of mitochondrial polarization is a factor contributing to the formation of memory-like NK cells. We cultured NKDim cells from an MD patient and compared them with NKDim cells derived from a HCMV[+] HD and HCMV[-] HD. Consistent with Figure 5D, we found that NKDim cells from the HCMV[+] HD could extensively expand during culture, whereas NKDim cells from the HCMV[+] MD patient could not (Figure 6D). Together, these results suggest that maintenance of fused mitochondria imparts cellular fitness to HCMV-conditioned adaptive NKDim cells.

Discussion

It is well appreciated that mitochondria orchestrate cellular metabolism; however, the importance of these organelles in NK cell biology is poorly understood. In this report, we identify distinct patterns of mitochondrial polarization in NKBr and NKDim subsets that explain their differential metabolic performances at steady state and after cytokine stimulation. Our analysis of mature NK cells in HCMV[+] and HCMV[-] donors together with patients with MD allows
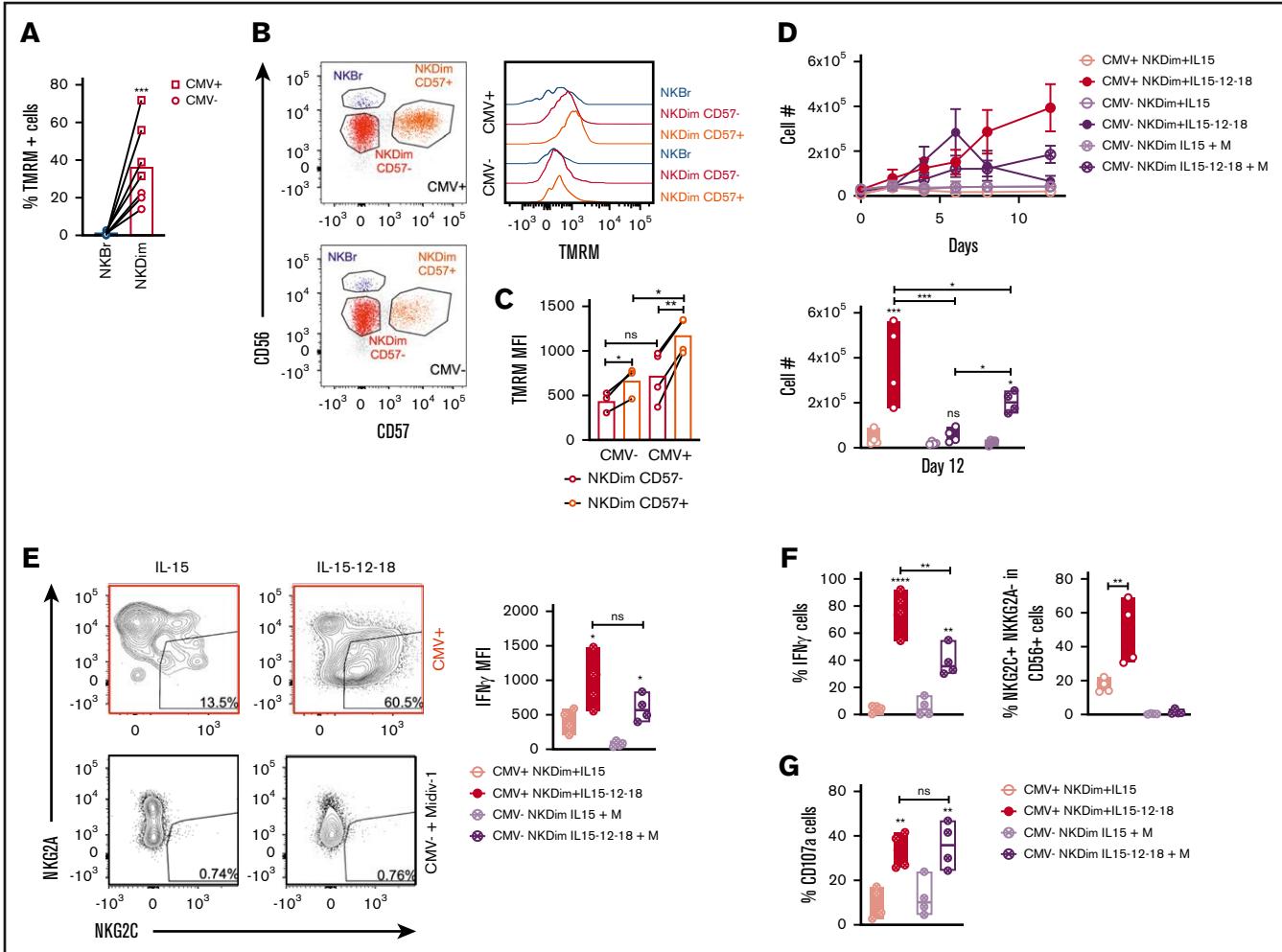
Figure 5. Mitochondrial fusion maintains NK cell survival and cellular fitness. (A) Percentage of TMRM$^+$ cells in NKBr and NKDim cells (data from 7 HDs). (B-C) Quantification of TMRM in CD57$^+$ NKDim and CD57$^-$ NKDim cells in CMV$^+$ and CMV$^-$ donors: representative plots (B) and quantification (C) (geometric mean fluorescence intensity [MFI]). (D-G) NKDim cells were cultured with IL-15 or IL-15/12/18 for 12 days. Mdivi-1 was added or not to NKDim cells from CMV$^-$ donors. (D) Growth curves of NKDim cells isolated from CMV$^+$ and CMV$^-$ HDs and cell numbers at end point. (E) Representative fluorescence-activated cell sorting (FACS) analysis of NKG2C and NKG2A and percentage of NKG2C$^+$NKG2A$^-$ cells in the indicated culture conditions at day 12. Quantification by FACS of IFN-γ and percentage of IFN-γ$^+$ cells (F) and CD107a$^+$ cells (G) at day 12 (data are mean ± SEM; data summarized from 3 independent experiments with at least 2 HDs each). $P > .05$ was considered not significant (ns). $*P < .05$, $**P < .01$, $***P < .001$, $****P < .0001$ using 2-way analysis of variance with Tukey's correction.

us to propose mitochondrial remodeling that regulates OXPHOS as an essential gatekeeper of NK cell effector functions.

Several reports have shown that acquisition of T-cell effector functions is strictly dependent on glycolysis. Exploring the energy requirements of NK cells, we similarly found that NKDim cells principally rely on glucose upon activation with IL-12/18. Interestingly, we found that NKBr cells consume both glutamine and FA upon activation, as described for efficient cytokine producers maintaining elevated cellular fitness.[34] NKBr cells are preferentially enriched in secondary lymphoid organs at low oxygen concentrations and restricted nutrient availability; therefore, they maintain high SRC upon cytokine stimulation for both longevity and rapid cytokine production. NKDim cells undergo metabolic reprogramming to glycolysis because they are preferentially recruited to sites of inflammation, where they rapidly get activated[43] and proliferate. How OXPHOS is related to cytokine production in

lymphocytes is a matter of debate. Moreover, this dichotomous response of NKBr vs NKDim cells mirrors observations made with central and effector memory T cells, respectively.[8] NKBr cells, which rely on FAs and maintain elevated SRC upon activation, resemble central memory T cells, whereas NKDim cells, metabolically reprogrammed to glycolysis, partially resemble effector memory T cells.[1,5,8] Moreover, together with cytokine-mediated activation, other environmental factors can have an impact on NK cell activation, such as the presence of target cells.[6] Unraveling the metabolic profiles of NK cell subsets upon different activation modes might help to better define the molecular basis of NK cell function.

At steady state, NKDim cells express OXPHOS genes, have elevated OCRs and ECARs, and have increased mitochondrial polarization compared with NKBr cells. We found that TMRM$^+$ NKDim cells were enriched in CD57$^+$ cells,[8] suggesting that
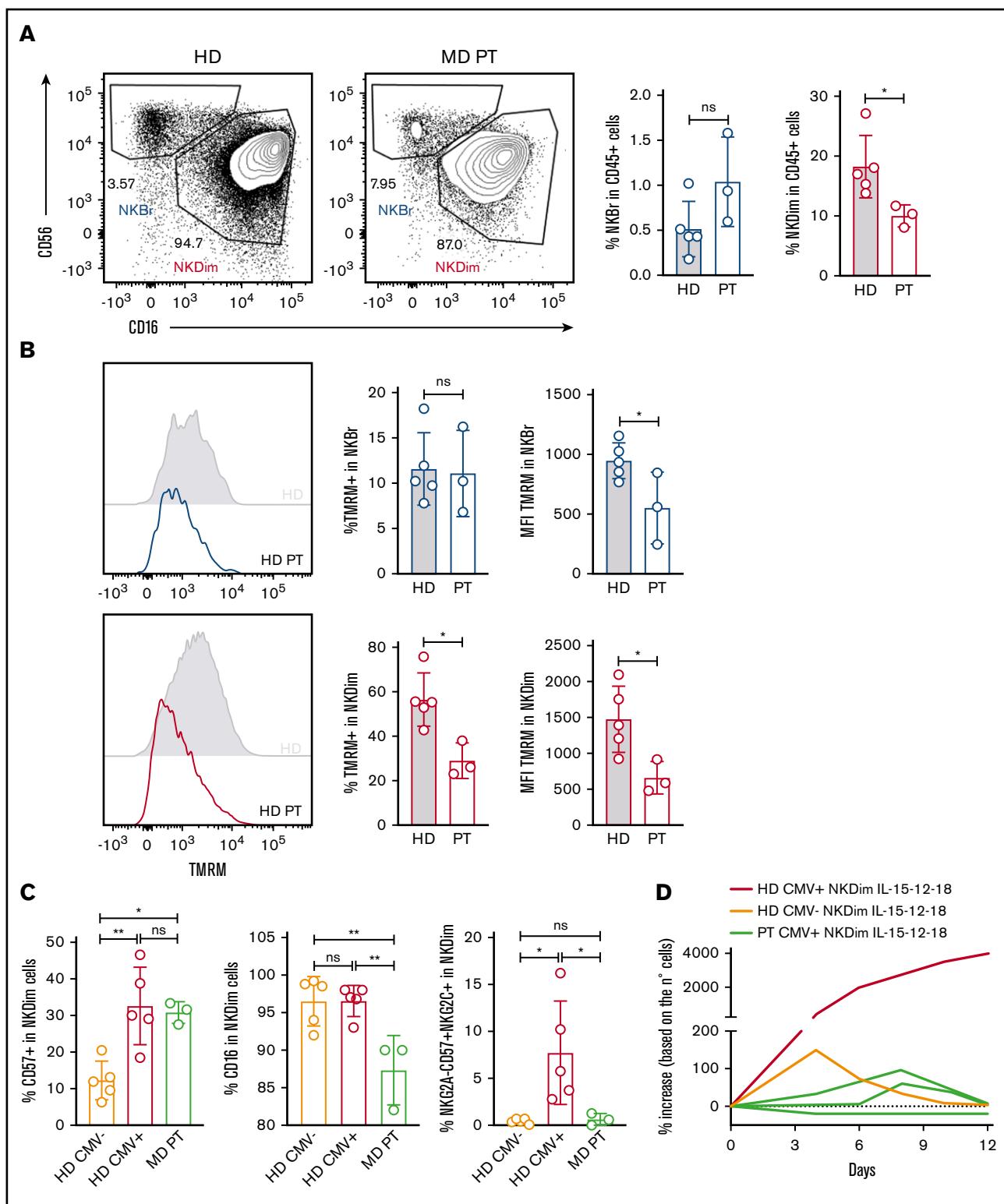
Figure 6. NK cells from MD patients have loss of memory-like NK cells and showed reduced cellular fitness. (A) Representative plots of NKBr and NKDim cells in HDs and MD patients with OPA1 mutation. Percentage of NKBr and NKDim cells in CD45+ cells. (B) Representative histograms of mitochondrial polarization in NKDim and NKBr cells comparing HDs and MD patients. Percentage of TMRM+ cells and TMRM intensity in NKBr and NKDim cells. (C) HDs and MD patients were compared with 5 CMV+ HDs by fluorescence-activated cell sorting (FACS). FACS analysis of the percentage of CD57+, CD16+, and CD57+NKG2A−NKG2C+ cells in NKDim cells. (D) Cells from 2 HDs and 3 MD patients were cultured in IL-15/12/18 for 12 days. Percentage of increase was calculated based on the number of cells (red, CMV+ HD; orange, CMV− HD; green, MD patients; data summarized from 2 independent experiments with at least 2 HDs each and 3 MD patients). $P > .05$ was considered not significant (ns). *$P < .05$, **$P < .01$ using 1-way analysis of variance with Tukey's correction.

mitochondrial polarization and OXPHOS are features of fully mature NK cells rather than markers of NKG2C$^+$ cells in HCMV$^+$ donors.[10] NKDim cells isolated from HCMV$^+$ donors were able to persist after long-term activation, whereas activated NKDim cells from HCMV$^-$ donors survived only in the presence of Mdivi-1. HCMV broadly affects NK cell biology via epigenetic changes[38,44] and favors mitochondrial biogenesis through the protein UL37.[45] This mitochondrial pathway provides a potential mechanistic explanation for the survival advantage observed in memory-like NK cells.

Still, additional metabolic reprogramming pathways independent of HCMV may operate to assure survival of mature NK cells. MD patients can manifest leukopenia and severe recurrent infections.[46] Deficiencies in the GTPase OPA1 are frequent in MDs,[47] and we found that OPA1-mutated patients had fewer NKDim cells and general loss of NK cell mitochondrial polarization. Similar to NK cells from HCMV$^+$ HDs, NK cells from HCMV$^+$ MD patients had higher levels of CD57 but very low frequencies of NKG2C$^+$ NK cells. Moreover, NKDim cells from MD patients expanded poorly in response to cytokines. These results indicate that mitochondrial fusion is essential for maintenance of adaptive NK cells and overall cellular fitness.

Our comprehensive metabolic analysis identifies mitochondrial polarization as a gatekeeper of NKBr and NKDim cell priming, activation, and function. Because OXPHOS and mitochondrial fusion promote long-term persistence and improve cytokine production by NK cells, enhancing this pathway may extend the scope and efficacy of NK cell–based therapies.

Acknowledgments

Authorship

Contribution: L.S. and J.P.D. conceptualized the study; L.S. was responsible for cell culture; L.S., C.C., A.T, and J.-M.D. performed fluorescence-activated cell sorting; S.M. and L.S. were responsible for Biomark analysis; P.E., C.B., and L.S. performed confocal microscopy; A.C., A.S., D.T., O.M, A.d.E., V.D., and N.T. provided resources; L.S. and J.P.D. wrote the paper; L.S. and J.P.D. provided funding; and J.P.D. supervised the study.

Conflict-of-interest disclosure: The authors declare no competing financial interests.

ORCID profiles: L.S., 0000-0001-8152-0611; J.-M.D., 0000-0001-6714-1308; P.E., 0000-0002-5933-094X; C.C., 0000-0002-4392-5498; A.T., 0000-0002-0698-8561; O.M., 0000-0002-9208-1527; C.B., 0000-0003-3477-9190; J.P.D.S., 0000-0002-7146-1862.

Correspondence: James P. Di Santo, Innate Immunity Unit, Inserm U1223, Institut Pasteur, 25 rue du Docteur Roux, 75724 Paris, France; e-mail: james.di-santo@pasteur.fr.

References

1. Pearce EL, Pearce EJ. Metabolic pathways in immune cell activation and quiescence. *Immunity*. 2013;38(4):633-643.

2. Chang C-H, Curtis JD, Maggi LB Jr., et al. Posttranscriptional control of T cell effector function by aerobic glycolysis. *Cell*. 2013;153(6):1239-1251.

3. Peng M, Yin N, Chhangawala S, Xu K, Leslie CS, Li MO. Aerobic glycolysis promotes T helper 1 cell differentiation through an epigenetic mechanism. *Science*. 2016;354(6311):481-484.

4. Bantug GR, Galluzzi L, Kroemer G, Hess C. The spectrum of T cell metabolism in health and disease. *Nat Rev Immunol*. 2018;18(1):19-34.

5. Nicoli F, Papagno L, Frere JJ, et al. Naïve CD8$^+$ T-cells engage a versatile metabolic program upon activation in humans and differ energetically from memory CD8$^+$ T-cells. *Front Immunol*. 2018;9:2736.

6. Freud AG, Mundy-Bosse BL, Yu J, Caligiuri MA. The broad spectrum of human natural killer cell diversity. *Immunity*. 2017;47(5):820-833.

7. Lanier LL, Le AM, Warner NL, Babcock GF. Subpopulations of human natural killer cells defined by expression of the Leu-7 (HNK-1) and Leu-11 (NK-15) antigens. *J Immunol*. 1983;131(4):1789-1796.

8. Collins PL, Cella M, Porter SI, et al. Gene regulatory programs conferring phenotypic identities to human NK cells. *Cell*. 2019;176(1-2):348-360.e12.

9. Crinier A, Milpied P, Escalière B, et al. High-dimensional single-cell analysis identifies organ-specific signatures and conserved NK cell subsets in humans and mice. *Immunity*. 2018;49(5):971-986.e5.

10. Cichocki F, Wu C-Y, Zhang B, et al. ARID5B regulates metabolic programming in human adaptive NK cells. *J Exp Med*. 2018;215(9):2379-2395.

11. Donnelly RP, Loftus RM, Keating SE, et al. mTORC1-dependent metabolic reprogramming is a prerequisite for NK cell effector function. *J Immunol*. 2014;193(9):4477-4484.

12. Keating SE, Zaiatz-Bittencourt V, Loftus RM, et al. Metabolic reprogramming supports IFN-□ production by CD56bright NK cells. *J Immunol*. 2016; 196(6):2552-2560.

13. Loftus RM, Assmann N, Kedia-Mehta N, et al. Amino acid-dependent cMyc expression is essential for NK cell metabolic and functional responses in mice. *Nat Commun*. 2018;9(1):2341.

14. Zheng X, Qian Y, Fu B, et al. Mitochondrial fragmentation limits NK cell-based tumor immunosurveillance. *Nat Immunol*. 2019;20(12):1656-1667.

15. Marçais A, Cherfils-Vicini J, Viant C, et al. The metabolic checkpoint kinase mTOR is essential for IL-15 signaling during the development and activation of NK cells. *Nat Immunol*. 2014;15(8):749-757.

16. Michelet X, Dyck L, Hogan A, et al. Metabolic reprogramming of natural killer cells in obesity limits antitumor responses. *Nat Immunol*. 2018;19(12): 1330-1340.

17. Rambold AS, Pearce EL. Mitochondrial dynamics at the interface of immune cell metabolism and function. *Trends Immunol*. 2018;39(1):6-18.

18. Cogliati S, Frezza C, Soriano ME, et al. Mitochondrial cristae shape determines respiratory chain supercomplexes assembly and respiratory efficiency. *Cell*. 2013;155(1):160-171.

19. Buck MD, O'Sullivan D, Pearce EL. T cell metabolism drives immunity. *J Exp Med*. 2015;212(9):1345-1360.

20. Kapnick SM, Pacheco SE, McGuire PJ. The emerging role of immune dysfunction in mitochondrial diseases as a paradigm for understanding immunometabolism. *Metabolism*. 2018;81:97-112.

21. Walker UA, Collins S, Byrne E. Respiratory chain encephalomyopathies: a diagnostic classification. *Eur Neurol*. 1996;36(5):260-267.

22. Lim AI, Li Y, Lopez-Lastra S, et al. Systemic human ILC precursors provide a substrate for tissue ILC differentiation. *Cell*. 2017;168(6):1086-1100.e10.

23. Manel N, Kinet S, Battini J-L, Kim FJ, Taylor N, Sitbon M. The HTLV receptor is an early T-cell activation marker whose expression requires de novo protein synthesis. *Blood*. 2003;101(5):1913-1918.

24. Laval J, Touhami J, Herzenberg LA, et al. Metabolic adaptation of neutrophils in cystic fibrosis airways involves distinct shifts in nutrient transporter expression. *J Immunol*. 2013;190(12):6043-6050.

25. Escoll P, Song O-R, Viana F, et al. Legionella pneumophila modulates mitochondrial dynamics to trigger metabolic repurposing of infected macrophages. *Cell Host Microbe*. 2017;22(3):302-316.e7.

26. Duchen MR, Surin A, Jacobson J. Imaging mitochondrial function in intact cells. *Methods Enzymol*. 2003;361:353-389.

27. Lucas M, Schachterle W, Oberle K, Aichele P, Diefenbach A. Dendritic cells prime natural killer cells by trans-presenting interleukin 15. *Immunity*. 2007; 26(4):503-517.

28. Gardiner CM, Finlay DK. What fuels natural killers? Metabolism and NK cell responses. *Front Immunol*. 2017;8:367.

29. Mavropoulos A, Sully G, Cope AP, Clark AR. Stabilization of IFN-gamma mRNA by MAPK p38 in IL-12- and IL-18-stimulated human NK cells. *Blood*. 2005;105(1):282-288.

30. Cooper MA, Fehniger TA, Caligiuri MA. The biology of human natural killer-cell subsets. *Trends Immunol*. 2001;22(11):633-640.

31. Jacobs R, Hintzen G, Kemper A, et al. CD56bright cells differ in their KIR repertoire and cytotoxic features from CD56dim NK cells. *Eur J Immunol*. 2001; 31(10):3121-3127.

32. O'Sullivan TE, Sun JC, Lanier LL. Natural killer cell memory. *Immunity*. 2015;43(4):634-645.

33. van der Windt GJW, Chang C-H, Pearce EL. Measuring bioenergetics in T cells using a Seahorse extracellular flux analyzer. *Curr Protoc Immunol*. 2016; 113:3.16B.1-3.16B.14.

34. van der Windt GJW, O'Sullivan D, Everts B, et al. CD8 memory T cells have a bioenergetic advantage that underlies their rapid recall ability. *Proc Natl Acad Sci USA*. 2013;110(35):14336-14341.

35. Gautam N, Sankaran S, Yason JA, Tan KSW, Gascoigne NRJ. A high content imaging flow cytometry approach to study mitochondria in T cells: MitoTracker Green FM dye concentration optimization. *Methods*. 2018;134-135:11-19.

36. Ferlazzo G, Thomas D, Lin S-L, et al. The abundant NK cells in human secondary lymphoid tissues require activation to express killer cell Ig-like receptors and become cytolytic. *J Immunol*. 2004;172(3):1455-1462.

37. Buck MD, O'Sullivan D, Klein Geltink RI, et al. Mitochondrial dynamics controls T cell fate through metabolic programming. *Cell*. 2016;166(1):63-76.

38. Gumá M, Angulo A, Vilches C, Gómez-Lozano N, Malats N, López-Botet M. Imprint of human cytomegalovirus infection on the NK cell receptor repertoire. *Blood*. 2004;104(12):3664-3671.

39. Hammer Q, Rückert T, Borst EM, et al. Peptide-specific recognition of human cytomegalovirus strains controls adaptive natural killer cells. *Nat Immunol*. 2018;19(5):453-463.

40. Lopez-Vergès S, Milush JM, Schwartz BS, et al. Expansion of a unique CD57^{+}NKG2Chi natural killer cell subset during acute human cytomegalovirus infection. *Proc Natl Acad Sci USA*. 2011;108(36):14725-14732.

41. Björkström NK, Lindgren T, Stoltz M, et al. Rapid expansion and long-term persistence of elevated NK cell numbers in humans infected with hantavirus. *J Exp Med*. 2011;208(1):13-21.

42. Holder KA, Lajoie J, Grant MD. Natural killer cells adapt to cytomegalovirus along a functionally static phenotypic spectrum in human immunodeficiency virus infection. *Front Immunol*. 2018;9:2494.

43. Melsen JE, Lugthart G, Lankester AC, Schilham MW. Human circulating and tissue-resident CD56(bright) natural killer cell populations. *Front Immunol*. 2016;7:262.

44. Schlums H, Cichocki F, Tesi B, et al. Cytomegalovirus infection drives adaptive epigenetic diversification of NK cells with altered signaling and effector function. *Immunity*. 2015;42(3):443-456.

45. Kaarbø M, Ager-Wick E, Osenbroch PØ, et al. Human cytomegalovirus infection increases mitochondrial biogenesis. *Mitochondrion*. 2011;11(6): 935-945.

46. Tarasenko TN, Pacheco SE, Koenig MK, et al. Cytochrome c oxidase activity is a metabolic checkpoint that regulates cell fate decisions during T cell activation and differentiation. *Cell Metab*. 2017;25(6):1254-1268.e7.

47. Carelli V, Musumeci O, Caporali L, et al. Syndromic parkinsonism and dementia associated with OPA1 missense mutations. *Ann Neurol*. 2015;78(1): 21-38.